PAPER

A Josephson junction with *h*-BN tunnel barrier: observation of low critical current noise

To cite this article: Jifa Tian *et al* 2021 *J. Phys.: Condens. Matter* **33** 495301

IOP Publishing Journal of Physics: Condensed Matter
J. Phys.: Condens. Matter **33** (2021) 495301 (6pp) https://doi.org/10.1088/1361-648X/ac268f

A Josephson junction with *h*-BN tunnel barrier: observation of low critical current noise

Jifa Tian[1,2,3,*], Luis A Jauregui[1,4], C D Wilen[5], Albert F Rigosi[3], David B Newell[3], R McDermott[5] and Yong P Chen[1,6,7,8,9,*]

[1] Department of Physics and Astronomy and Birck Nanotechnology Center, Purdue University, West Lafayette, IN 47907, United States of America
[2] Department of Physics and Astronomy, University of Wyoming, Laramie, WY 82071, United States of America
[3] National Institute of Standards and Technology, Gaithersburg, MD 20899, United States of America
[4] Department of Physics and Astronomy, University of California, Irvine, CA 92697, United States of America
[5] Department of Physics, University of Wisconsin-Madison, Madison, WI 53706, United States of America
[6] Purdue Quantum Science and Engineering Institute, Purdue University, West Lafayette, IN 47907, United States of America
[7] School of Electrical and Computer Engineering, Purdue University, West Lafayette, IN 47907, United States of America
[8] Institute of Physics and Astronomy and Villum Centers for Dirac Materials and for Hybrid Quantum Materials, Aarhus University, 8000 Aarhus-C, Denmark
[9] WPI-AIMR International Research Center for Materials Sciences, Tohoku University, Sendai 980-8577, Japan

E-mail: jtian@uwyo.edu and yongchen@purdue.edu

Received 22 July 2021, revised 30 August 2021
Accepted for publication 14 September 2021
Published 1 October 2021

Abstract

Decoherence in quantum bits (qubits) is a major challenge for realizing scalable quantum computing. One of the primary causes of decoherence in qubits and quantum circuits based on superconducting Josephson junctions is the critical current fluctuation. Many efforts have been devoted to suppressing the critical current fluctuation in Josephson junctions. Nonetheless, the efforts have been hindered by the defect-induced trapping states in oxide-based tunnel barriers and the interfaces with superconductors in the traditional Josephson junctions. Motivated by this, along with the recent demonstration of 2D insulator *h*-BN with exceptional crystallinity and low defect density, we fabricated a vertical $NbSe_2$/*h*-BN/Nb Josephson junction consisting of a bottom $NbSe_2$ superconductor thin layer and a top Nb superconductor spaced by an atomically thin *h*-BN layer. We further characterized the superconducting current and voltage (I–V) relationships and Fraunhofer pattern of the $NbSe_2$/*h*-BN/Nb junction. Notably, we demonstrated the critical current noise ($1/f$ noise power) in the *h*-BN-based Josephson device is at least a factor of four lower than that of the previously studied aluminum oxide-based Josephson junctions. Our work offers a strong promise of *h*-BN as a novel tunnel barrier for high-quality Josephson junctions and qubit applications.

Keywords: Josephson junctions, boron nitride, critical current noise

(Some figures may appear in colour only in the online journal)

* Authors to whom any correspondence should be addressed.

1. Introduction

Josephson junctions underlie the operations of many superconductor-based device applications ranging from superconducting quantum interference devices (SQUIDs) to superconducting quantum bits (qubits) for quantum computing [1, 2]. A representative superconductor–insulator–superconductor (S/I/S) Josephson junction normally consists of two superconductors separated by a thin insulator as a tunnel barrier. Typically, the tunnel barriers in the S/I/S junctions are made of a thin metal oxide layer [2], such as aluminum oxide (AlO_x) [3]. One of the grand challenges of realizing scalable quantum computing using such a mesoscopic S/I/S junction device is the minimization of decoherence of qubits [4, 5]. It has been shown that the coherence time of qubits in S/I/S Josephson junctions is largely affected by the quality of the individual materials [6–9], particularly, the insulating spacer as well as the interfaces between the insulating spacer and its adjacent superconductors, where charge trapping states can inevitably exist. For example, one of the serious problems is the critical-current fluctuation caused by the charge trapping at the defect sites in the S/I/S Josephson junctions [4, 5, 10–12]. In recent years, a long-standing goal in this field is to create a high-quality and defect-free insulating spacer that may lead to improved properties of the superconducting Josephson junctions.

Ever since the mechanical exfoliation of atomically thin graphene layers from bulk graphite [13, 14] and their deposition or dry-transferring on various substrates [14], significant progress has also been made in other two-dimensional (2D) materials, including examples such as insulating hexagonal boron nitride (*h*-BN) [15, 16], superconducting niobium diselenide ($NbSe_2$) [6, 17], semiconducting molybdenum disulfide (MoS_2) [18, 19] and black phosphorene (BP) [20], etc. An attractive merit of using 2D insulators and semiconductors as tunnel barriers in high-quality Josephson junctions is that such 2D materials can be highly crystalline, atomically thin, and nearly defect-free. Recently, notable progress has been made in making designable Josephson junctions using insulating/semiconducting 2D materials. For instance, the Josephson effect in Al/MoS_2/Al tunnel junctions using a MoS_2 thin layer as the tunnel barrier has been recently demonstrated [19]. People have developed an *in situ* technique to fabricate Nb/BP/Nb Josephson junctions and demonstrated good interfacial properties between Nb and BP by the Josephson effect [21]. Recently, 2D magnetic insulators (MIs) have also been used to fabricate high-quality magnetic Josephson junctions consisting of 2D superconductor/2D MI/2D superconductor van der Waals (vdW) heterostructures [22–24]. On the other hand, *h*-BN as the first discovered 2D insulator with a large band gap has attracted extensive attention [16, 25, 26], promising an ideal candidate for making single crystalline and defect-free insulating spacers for Josephson junctions. However, quantitatively analyzing the quality of the Josephson junction devices with an atomically thin *h*-BN layer is still missing. Specifically, how the 2D insulator tunnel barrier affects the critical current noise in the Josephson junctions remains unanswered. In the present study, we have fabricated a vertical $NbSe_2$/*h*-BN/Nb Josephson junction (figure 1(a)) using a bilayer *h*-BN as the insulating spacer (tunnel barrier) and systematically studied its transport characteristics. Our results demonstrate clear Josephson transport properties in the $NbSe_2$/*h*-BN/Nb junction device. We further measured the critical current fluctuations with a $1/f$ spectral density at low-frequency in the $NbSe_2$/*h*-BN/Nb Josephson device. We find that the critical current noise in the *h*-BN based Josephson device is at least a factor of four lower than the $1/f$ noise power of the previously studied aluminum oxide-based junctions [10].

2. Results and discussion

We first measured the temperature dependences of the resistances (R) from different parts of the Josephson junction, including the two superconductors (Nb and $NbSe_2$) and the $NbSe_2$/*h*-BN/Nb junction itself (figure 1(d)), respectively. As shown in figure 2(a), all three R vs T curves show a sharp transition from a normal resistive state to a zero-resistance superconducting state at the critical temperatures T_c's, indicating a clearly developed superconductivity. The extracted critical temperatures T_c's of Nb, $NbSe_2$, and $NbSe_2$/*h*-BN/Nb junction (figure 2(a)) are ≈7 K, 6 K, and 5 K, respectively. We note that the critical temperatures of Nb (7 K) and $NbSe_2$ (6 K) in our device are slightly lower than their bulk values (9.25 K for Nb and 7.2 K for $NbSe_2$), but higher than the critical temperature T_c (≈5 K) of the $NbSe_2$/*h*-BN/Nb Josephson junction. Our temperature dependences of the Josephson junction device exhibit the direct signatures of superconductivity and Josephson coupling in the $NbSe_2$/*h*-BN/Nb junction through the *h*-BN tunnel barrier. We further note that, compared to other tunnel devices using atomically thin *h*-BN layers [16, 27], the normal resistance of the $NbSe_2$/*h*-BN/Nb junction is relatively small due to the possible pinholes or defects created in the *h*-BN spacer during the sputtering procedure.

We further studied the current–voltage (I–V) characteristics of the $NbSe_2$/*h*-BN/Nb Josephson junction at $T = 300$ mK as shown in figure 2(b). The I–V curves not only exhibit a hysteresis loop as the bias current is swept back and forth, but also show a clear zero-voltage state when the bias current is less than the critical current I_c. As the bias current I is increased above the critic current I_c, a finite voltage can be measured, indicating that the junction transitions to its normal resistive states, showing the typical behavior of an underdamped Josephson junction. From figure 2(b), we can further extract the Josephson critical current (I_c) of this device to be ≈120 μA at $T = 300$ mK. The corresponding critical current density is 2800 A cm^{-2} with a junction area of 4.25 μm^2. In addition to the hysteresis around the critical current of $I_c = 120$ μA, we also observed additional voltage jumps around $I = 140$ and 175 μA as shown in figure 2(b). We attribute these features to breaking of superconductivity (at such high currents) in the $NbSe_2$ and Nb layers rather than the $NbSe_2$/*h*-BN/Nb junction itself. All of our I–V results demonstrate a clear Josephson coupling in our $NbSe_2$/*h*-BN/Nb junction device through the atomically thin *h*-BN spacer,

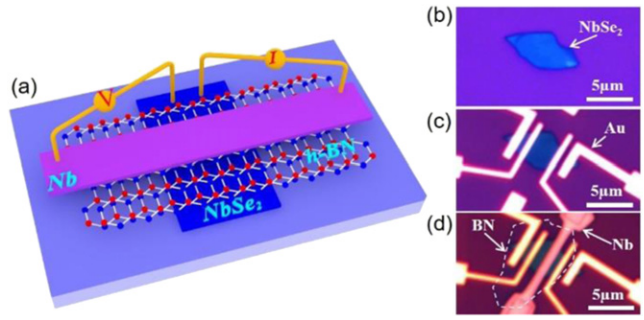

Figure 1. A vertical $NbSe_2$/*h*-BN/Nb Josephson junction. (a) Schematic illustration of a vertical $NbSe_2$/*h*-BN/Nb Josephson junction using a bilayer *h*-BN as the spacer (tunnel barrier). (b)–(d) Device fabrication process of the vertical $NbSe_2$/*h*-BN/Nb Josephson junction. (b) A $NbSe_2$ thin flake with thickness of 15 nm exfoliated on a Si/SiO_2 substrate. (c) Four Ti/Au contacts fabricated on the $NbSe_2$ thin flake. (d) The final device of the $NbSe_2$/*h*-BN/Nb Josephson junction after dry-transferring a thin *h*-BN layer on top of the $NbSe_2$ thin flake and followed by sputtering a Nb top electrode, with a junction area of 4.25 μm^2. The white dashed line highlights the perimeter of the *h*-BN thin flake. The thickness of the *h*-BN flake is ≈1 nm.

which introduces a discontinuity in the superconducting order parameter in the Josephson effect.

We also examined another hallmark of the Josephson effect, the Fraunhofer effect, in the $NbSe_2$/*h*-BN/Nb junction. It is known that the application of a magnetic field in the junction plane of a Josephson junction induces a gradient in the phase difference between the superconductors, thereby inducing a variation in the critical current I_c (which is driven by the phase difference). In our measurements, an in-plane magnetic field was applied along the long diagonal direction of the bottom $NbSe_2$ layer (figure 1(b)). The in-plane magnetic field dependence of the I–V curve measured at $T = 1.4$ K is shown in figure 3. The critical current I_c exhibits an approximately periodical modulation by the applied magnetic field. We further extracted a periodicity $H_0 \approx 50$ mT from the Fraunhofer-like diffraction pattern (figure 3). Theoretically, based on the device geometry of our device, we can estimate the expected periodicity H_0 $(=\Phi_0/[W(d_t + \lambda_L + \lambda'_L)]) = 13.5$ mT, which is the magnetic field corresponding to a flux quantum $\Phi_0 = h/2e$ threading the junction cross section area $A = W(d_t + \lambda_L + \lambda'_L) = 0.153\ \mu m^2$. Here, $W = 3.4\ \mu m$ is defined by the width of the bottom electrode ($NbSe_2$), $d_t = 1$ nm is the thickness of the *h*-BN, and $\lambda_L = 39$ nm and $\lambda'_L = 5$ nm are the London penetration depths (in the direction perpendicular to the sample surface) of bulk Nb [28] and $NbSe_2$ [29], respectively. We find that the measured periodicity H_0 (≈50 mT) from the Josephson effect is ≈3.7 times larger than the theoretically calculated periodicity based on our device geometry and London penetration depths estimated from the bulk values. We speculate that the extended periodicity H_0 observed in our $NbSe_2$/*h*-BN/Nb device can be caused by several factors: for instance, (1) the effective width of the Josephson junction can be shorter than the sample width (3.4 μm); (2) the London penetration depths of the two superconductors are highly dependent on their growth conditions and can be significantly different from the reported bulk values that we used in our estimations. If the width of the junction is fixed to 3.4 μm, the sum of London penetration depths $(\lambda_L + \lambda'_L)$ of the two superconductors based on the actual H_0 is expected to be ≈11 nm only. We further find that the observed I_c modulation can be fitted to an expected expression of the Josephson junction Fraunhofer pattern $I_c(H) = I_c(0)\left|\frac{\sin\frac{\pi H}{H_0}}{\frac{\pi H}{H_0}}\right|$, where $I_c(0) = 120\ \mu A$ is the critical current at zero magnetic field. As shown in figure 3, this fitting curve matches reasonably well with the contour of the measured pattern. In addition, the observed single-slit interference-like dependence of I_c on the magnetic field further confirms that the supercurrent of our $NbSe_2$/*h*-BN/Nb junction originates from the Josephson effect through the *h*-BN tunnel barrier, rather than any direct shorting between the Nb and $NbSe_2$ superconductors.

In a conventional S/I/S Josephson junction, fluctuating conduction channels cause the I_c to fluctuate with a $1/f$ power spectrum $S_{I_c} = S^*_{I_c}(1\ \text{Hz})/f$. It has been suggested that the critical current noise is dominated by microscopic defects in the amorphous insulating barrier of the junction or at the disordered metal–insulator interface. In a superconducting qubit, any fluctuation in I_c modulates the energy level separation between the qubit 0 and 1 states; therefore low-frequency I_c noise is a potential source of qubit dephasing. These fluctuations also limit the sensitivity of Josephson devices such as SQUID magnetometers. Previous studies have found critical current noise $S^*_{I_c}(1\ \text{Hz}) = (10^{-6}I_c)^2$ for 100 μm^2 conventional (AlO_x based) junctions at 4 K; moreover, $S^*_{I_0}(1\ \text{Hz})/I_c^2$ scales inversely with junction area and as the square of temperature [10–12].

We have performed the I_c noise characterization on the NbSe/*h*-BN/Nb Josephson junction at $T = 3$ K. In the experiment, the NbSe/*h*-BN/Nb junction was voltage biased and a separate dc SQUID circuit was used to monitor the current through the junction. The representative noise spectrum is presented in figure 4. We measured a current noise amplitude at 1 Hz of 20 pA $Hz^{-1/2}$ A^{-1} in the $NbSe_2$/*h*-BN/Nb Josephson junction with a lateral junction area of 4.25 μm^2. Separate tests reveal that this noise is dominated by the noise of the measurement system and, thus, this result represents only an upper bound on the critical current noise of the junction. We note that, such an upper limit, though, is already a factor of 4 lower than that in the conventional oxide-based Josephson junctions (after proper scaling of junction's critical current, area, and temperature) [10–12]. Thus, our result demonstrates the strong promise of *h*-BN as an improved tunnel barrier for Josephson quantum devices and qubit applications. We note that, in order to circumvent the noise contribution of the readout circuit and access the true intrinsic noise of the *h*-BN junction, one may further decrease the area of the *h*-BN junction in order to enhance the magnitude of fluctuating conductance channels relative to the overall junction conductance. We further note that in our current devices, defects or pinholes may be created in the *h*-BN during Nb sputtering. It is expected that the defects and the noise of the *h*-BN-based Josephson junction can be further reduced by replacing the Nb contact with a 2D superconductor layer to form an all-vdW Josephson junction, where clean interfaces in the Josephson junctions may be achieved.

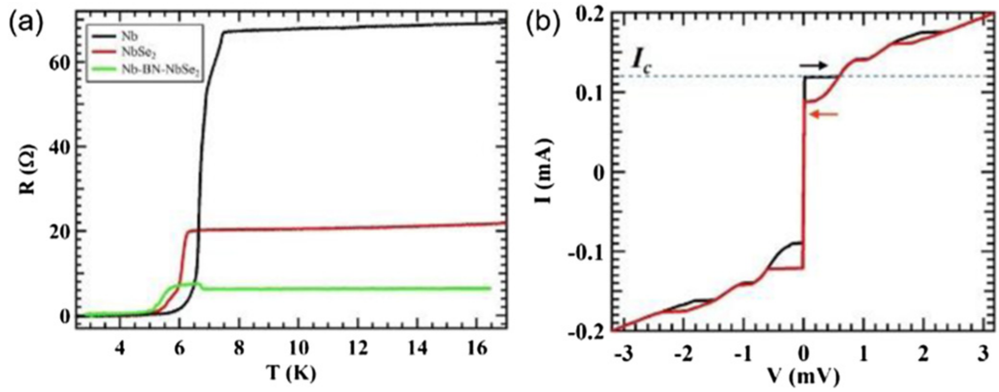

Figure 2. Electrical characterization of superconductivity in the $NbSe_2$/*h*-BN/Nb Josephson junction: (a) resistance (R) vs temperature (T) measured on Nb, $NbSe_2$, and the $NbSe_2$/*h*-BN/Nb junction, respectively. (b) Current–voltage (I–V) curves of the $NbSe_2$/h-BN/Nb Josephson junction measured by sweeping the bias current at $T = 300$ mK, featuring a superconducting critical current $I_c = 120\ \mu$A. Arrows indicate the sweep directions of the current.

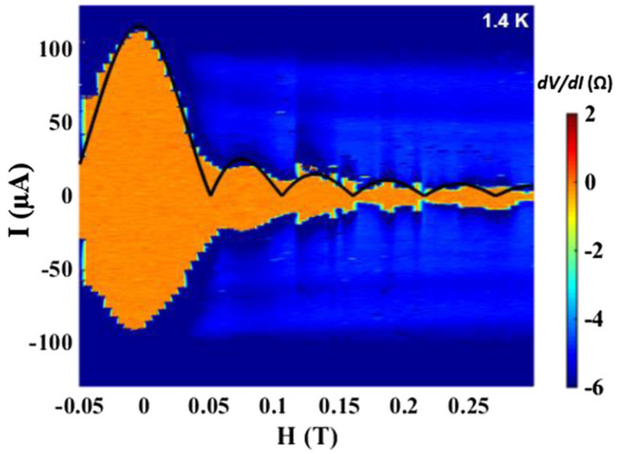

Figure 3. Measurement of Fraunhofer pattern in the $NbSe_2$/*h*-BN/Nb Josephson junction. Color plot of dV/dI as a function of the bias current I and in-plane magnetic fields at $T =$ 1.4 K, showing a characteristic Fraunhofer-like diffraction pattern with fitting (solid line).

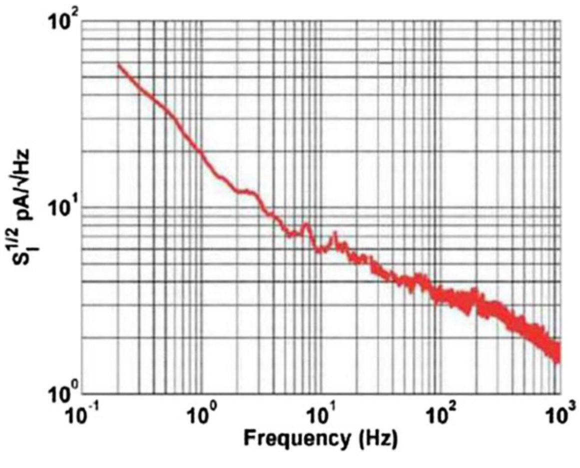

Figure 4. The critical current noise spectra of the $NbSe_2$/*h*-BN/Nb Josephson junction measured at $T = 3$ K. The system noise floor is dominated by the noise of the SQUID-based measurement circuit used to monitor the critical current fluctuations and thus represents an upper limit on the actual critical current noise of the *h*-BN-based junction.

3. Conclusion

In conclusion, we have fabricated a vertical S/I/S Josephson junction device using a single-crystalline *h*-BN layer as the insulating spacer between two superconductors ($NbSe_2$ and Nb). Through the transport studies, we have observed well developed Josephson effect in the $NbSe_2$/*h*-BN/Nb junction device. We further demonstrated that, by using the single crystalline *h*-BN in the S/I/S Josephson junction, the critical current noise of the device is at least a factor of 4 lower than the $1/f$ noise power of the previously studied aluminum oxide-based Josephson junctions. Our results pave a possible way to reduce the noise and improve the sensitivity of SQUID magnetometers, as well as to extend the coherence time of Josephson junctions-based qubits for quantum computing applications.

4. Methods

4.1. Device fabrication

We fabricated the $NbSe_2$/*h*-BN/Nb Josephson junctions incorporating a single-crystalline *h*-BN spacer and two superconductors ($NbSe_2$, which is a 2D/vdW superconductor, and Nb). The $NbSe_2$ thin flakes (10 nm to 30 nm) were mechanically exfoliated from a 2H-$NbSe_2$ bulk crystal ($T_c \approx 7.2$ K) and transferred on a SiO_2 (300 nm)/Si (heavily doped) substrate (figure 1(b)). To prevent surface oxidation of the $NbSe_2$ layer, a layer of polymethyl methacrylate (PMMA) e-beam resist was immediately spin-coated on the substrate. Then, a few windows were opened in the PMMA layer using the standard e-beam lithography. Four Ti/Au (10 nm/60 nm) metal contacts (figure 1(c)) were deposited on the $NbSe_2$ flake using an e-beam evaporator. To prepare the *h*-BN tunnel barrier (typically ≈1–2 nm-thick, characterized by atomic force microscopy and optical microscopy), we exfoliated the atomically thin layer from the *h*-BN bulk crystals (HQ graphene) on another SiO_2 (100 nm)/Si substrate. After the lift-off step of the $NbSe_2$ device fabrication, the selected *h*-BN flake was transferred on top of the $NbSe_2$ flake using a dry-transfer technique (figures 1(c) and (d)) [30]. To minimize the possible surface oxidation of the $NbSe_2$ layer, the whole transfer process was limited to 30 min. Finally, the top superconductor Nb (80 nm thick) was made by another round of e-beam lithography and followed by sputter deposition. The final $NbSe_2$/*h*-BN/Nb Josephson device is shown in figure 1(d).

4.2. Device characterization

To study the transport characteristics of the $NbSe_2$/*h*-BN/Nb Josephson junction, the device ($NbSe_2 \approx 15$ nm; Nb ≈ 80 nm) was cooled in a variable temperature insert with a base temperature of $T = 1.5$ K or a He-3 cryostat with a base temperature of $T = 300$ mK. All the resistance measurements were using a typical four-terminal configuration. We characterized the temperature dependences of the resistances from different parts of the $NbSe_2$/*h*-BN/Nb Josephson junction. We further measured the I–V characteristics of the Josephson junction. The measurement circuit lines used for the I–V characterizations were electrically filtered by two-stage low-pass RC filters, with a cutoff frequency of $\approx$10 kHz, in combination with another set of RC filters and π-type low-pass LC filters with a cutoff frequency of 10 MHz at room temperature. To further measure the critical current noise, the devices were cooled to 3 K using a pulse tube cooler (which is part of an adiabatic demagnetization refrigerator system). The $NbSe_2$/*h*-BN/Nb Josephson junction was voltage biased and fluctuations in the critical current were measured by an auxiliary Nb-AlO_x-Nb SQUID [31]. Here, the integrated input coil of the readout SQUID was wired in series with the $NbSe_2$/*h*-BN/Nb junction and the readout SQUID was operated in a flux-locked loop with flux modulation at 100 kHz. The noise floor was dominated by the added noise of the measurement system, so we are only able to set an upper bound on the critical current noise of the Josephson junction.

Acknowledgments

We acknowledge valuable discussions with C C Yu and experimental help from L Rokhinson. We acknowledge partial support during various stages of the work from DARPA MESO program (Award N66001-11-1-4107), NSF (Award EFMA-1641101), and JSPS Kakenhi (18H03858). JT also acknowledges DOE, Office of Basic Energy Sciences, Division of Materials Sciences and Engineering for financial support under Award DE-SC0021281. YPC also acknowledges support from DOE, Office of Science through the Quantum Science Center (QSC), a National Quantum Information Science Research Center. JT and YPC acknowledge support from the U.S. Department of Commerce, National Institute of Standards and Technology under the financial assistance award 70NANB12H184. The authors thank C-I Liu, G Fitzpatrick, A L Levy, E C Benck, and the NIST Editorial Review Board for assistance with the internal NIST review process. Commercial equipment, instruments, and materials are identified in this paper in order to specify the experimental procedure adequately. Such identification is not intended to imply recommendation or endorsement by the National Institute of Standards and Technology or the United States government, nor is it intended to imply that the materials or equipment identified are necessarily the best available for the purpose.

Data availability statement

The data that support the findings of this study are available upon reasonable request from the authors.

ORCID iDs

Jifa Tian https://orcid.org/0000-0003-2921-470X
Albert F Rigosi https://orcid.org/0000-0002-8189-3829
R McDermott https://orcid.org/0000-0001-5677-8637
Yong P Chen https://orcid.org/0000-0002-7356-4179

References

[1] Makhlin Y, Schön G and Shnirman A 2001 *Rev. Mod. Phys.* **73** 357–400
[2] Clarke J and Wilhelm F K 2008 *Nature* **453** 1031
[3] Schulze H, Behr R, Müller F and Niemeyer J 1998 *Appl. Phys. Lett.* **73** 996–8
[4] van Harlingen D J, Robertson T L, Plourde B L T, Reichardt P A, Crane T A and Clarke J 2004 *Phys. Rev.* B **70** 064517
[5] Ansari M H and Wilhelm F K 2011 *Phys. Rev.* B **84** 235102
[6] Xi X, Zhao L, Wang Z, Berger H, Forró L, Shan J and Mak K F 2015 *Nat. Nanotechnol.* **10** 765
[7] McDermott R 2009 *IEEE Trans. Appl. Supercond.* **19** 2–13
[8] Oliver W D and Welander P B 2013 *MRS Bull.* **38** 816–25
[9] Zeng L J, Nik S, Greibe T, Krantz P, Wilson C M, Delsing P and Olsson E 2015 *J. Phys. D: Appl. Phys.* **48** 395308
[10] Nugroho C D, Orlyanchik V and van Harlingen D J 2013 *Appl. Phys. Lett.* **102** 142602
[11] Mück M, Korn M, Mugford C G A, Kycia J B and Clarke J 2005 *Appl. Phys. Lett.* **86** 012510
[12] Eroms J, van Schaarenburg L C, Driessen E F C, Plantenberg J H, Huizinga C M, Schouten R N, Verbruggen A H, Harmans C J P M and Mooij J E 2006 *Appl. Phys. Lett.* **89** 122516
[13] Novoselov K S, Geim A K, Morozov S V, Jiang D, Zhang Y, Dubonos S V, Grigorieva I V and Firsov A A 2004 *Science* **306** 666–9
[14] Novoselov K S, Mishchenko A, Carvalho A and Castro Neto A H 2016 *Science* **353** aac9439
[15] Dean C R *et al* 2010 *Nat. Nanotechnol.* **5** 722
[16] Britnell L *et al* 2012 *Nano Lett.* **12** 1707–10
[17] Yabuki N, Moriya R, Arai M, Sata Y, Morikawa S, Masubuchi S and Machida T 2016 *Nat. Commun.* **7** 10616
[18] Radisavljevic B, Radenovic A, Brivio J, Giacometti V and Kis A 2011 *Nat. Nanotechnol.* **6** 147–50
[19] Lee K-H *et al* 2019 *Nano Lett.* **19** 8287–93
[20] Li L, Yu Y, Ye G J, Ge Q, Ou X, Wu H, Feng D, Chen X H and Zhang Y 2014 *Nat. Nanotechnol.* **9** 372–7
[21] Chen W *et al* 2019 *Supercond. Sci. Technol.* **32** 115005
[22] Idzuchi H *et al* 2020 arXiv:2012.14969
[23] Kang K, Jiang S, Berger H, Watanabe K, Taniguchi T, Forró L, Shan J and Mak K F 2021 arXiv:2101.01327
[24] Ai L *et al* 2021 arXiv:2101.04323
[25] Kamalakar M V, Dankert A, Bergsten J, Ive T and Dash S P 2014 *Sci. Rep.* **4** 6146
[26] Fu W, Makk P, Maurand R, Bräuninger M and Schönenberger C 2014 *J. Appl. Phys.* **116** 074306
[27] Dankert A, Venkata Kamalakar M, Wajid A, Patel R S and Dash S P 2015 *Nano Res.* **8** 1357–64

[28] Maxfield B W and McLean W L 1965 *Phys. Rev.* **139** A1515–22
[29] Fletcher J D, Carrington A, Diener P, Rodière P, Brison J P, Prozorov R, Olheiser T and Giannetta R W 2007 *Phys. Rev. Lett.* **98** 057003
[30] Andres C-G, Michele B, Rianda M, Vibhor S, Laurens J, van der Zant H S J and Gary A S 2014 *2D Mater.* **1** 011002
[31] Sendelbach S, Hover D, Kittel A, Mück M, Martinis J M and McDermott R 2008 *Phys. Rev. Lett.* **100** 227006